Published OnlineFirst September 7, 2010; DOI:10.1158/1078-0432.CCR-10-0407

Table 1. Microarray analysis of metastatic lesions in liver (Cont'd)

Rank	Reported to be hypoxia-inducible genes		Reported as prognostic factor in cancers	Microarray data of five CRC cell lines (induction level under hypoxic condition)
	Well-known†	Limited number of reports		Median fold (range)
1				1.1 (0.86-1.82)
2				1.17 (0.4-1.91)
3	Yes		Yes	1.21 (0.95-5.44)
4				0.7 (1.08-1.22)
5	Yes		Yes	2.17 (0.85-4.04)
6		Yes		3.17 (2-7.42)
7			—	1.42 (0.4-2.95)
8		Yes	Yes	0.83 (0.69-3.5)
9		Yes		1.82 (1.02-8.33)
10				0.82 (0.41-2.9)
11				1.51 (0.16-3.25)
12	Yes		Yes	0.74 (0.28-1.22)
13				0.91 (0.7-3.93)
14				1.16 (0.34-2.74)
15				1.39 (0.62-1.86)
16				1.39 (1.02-2.26)
17	Yes		Yes	1.75 (1.25-2.39)
18				0.67 (0.62-1.28)
19				1.1 (0.49-1.45)
20				0.96 (0.72-1.32)
21	Yes		Yes‡	1.59 (0.75-1.9)
22				1.37 (0.8-2.6)
23				0.56 (0.17-2.7)
24				0.81 (0.44-6.3)
25				1.41 (0.98-1.54)
26		Yes	Yes	1.01 (0.87-1.18)
27		Yes		2.76 (1.69-8.15)
28				0.5 (0.33-1.03)
29				1.76 (1.55-5.05)
30	Yes		Yes	1.29 (1.02-1.92)

*Unknown genes contain genes such as ESTs and hypothetical proteins, whose function is unclear.

†Already well known as hypoxia-inducible gene; >50 publications related to hypoxia appear in the database of the National Library of Medicine (PubMed).

‡There is one reported as a prognostic factor in human cancer (ovarian cancer: $n = 60$, only in univariate analysis; ref. 35).

each; Fig. 4A). Similar results were obtained at MOI of 50 and 25 in both cells (data not shown). Treatment of established tumor xenografts, derived from the two cell lines, with intratumoral injection (four times) of Ad-AS JMJD1A significantly inhibited *in vivo* tumor growth when compared with the control groups ($P < 0.05$ for each; Fig. 4B).

Discussion

JMJD1A was initially identified in a testis cDNA library in 1991 (33), but its biological function has not yet been clarified. Studies gradually uncovered the roles of JMJD1A. JMJD1A is a histone H3 Lys^9 demethylase that causes transcriptional activation of certain downstream target genes (12–14), and it plays a role in embryonic stem cell differentiation (34) and spermatogenesis (13). Here, we report for the first time that JMJD1A could be an important prognostic factor for patients with CRC.

In a chronically hypoxic microenvironment, cancer cells undergo genetic and adaptive changes that allow them to become more clinically aggressive and to develop resistance to irradiation and chemotherapy (8, 9, 35). An efficient therapeutic strategy against those cell types is essential to overcome cancer, and we aimed to determine a novel molecular target that is induced under *in vivo* hypoxic conditions.

Published OnlineFirst September 7, 2010; DOI:10.1158/1078-0432.CCR-10-0407

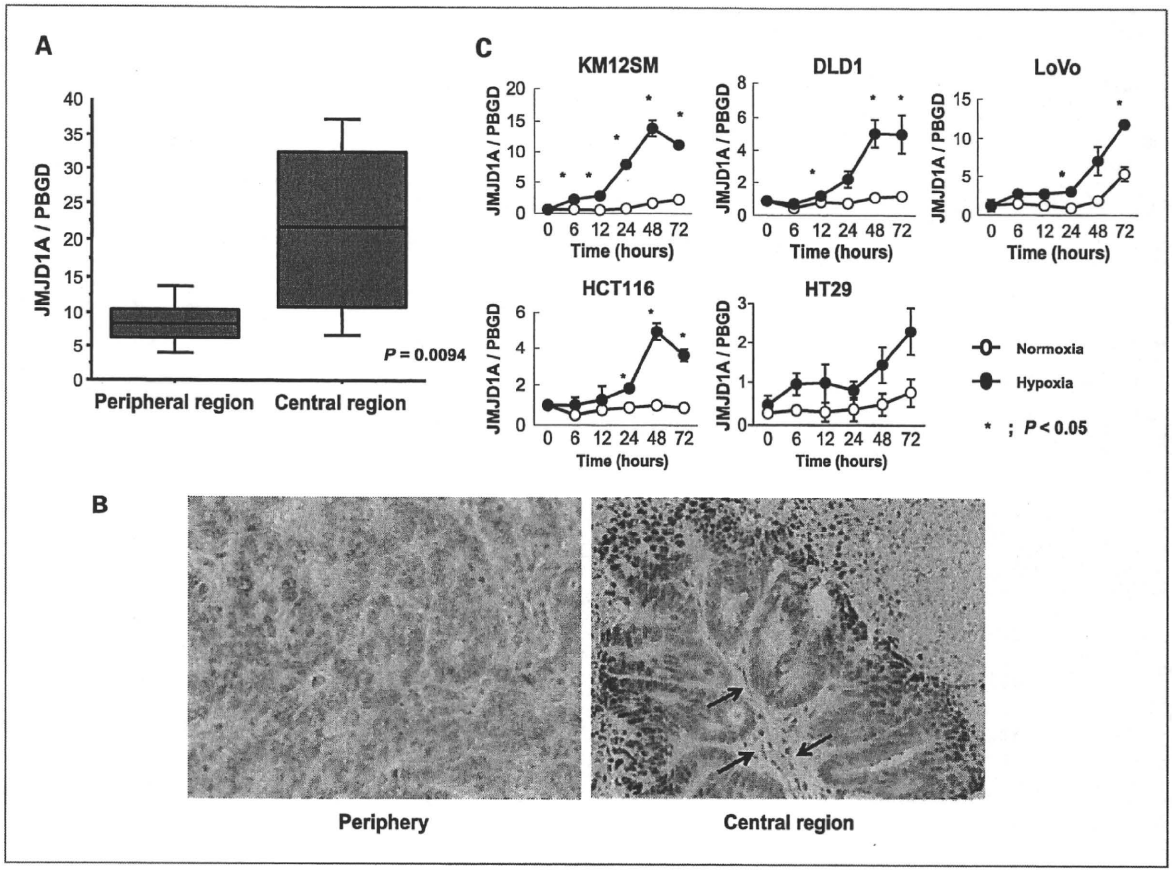

Fig. 2. Expression of JMJD1A in liver metastatic lesions. A, RT-PCR analysis indicated that JMJD1A expression had a 2.52-fold higher induction in the central region ($n = 12$; $P = 0.0094$). B, JMJD1A expression in tumor cells (brown) increased from the periphery to the central region. Black arrows indicate the tumor vessels. The intensity of JMJD1A staining was enhanced 80 μm from the tumor vessel. Magnification, ×200. C, quantitative analysis of JMJD1A gene expression in CRC cell lines under hypoxic conditions. In the majority of CRC cell lines, JMJD1A mRNA expression increased progressively under hypoxic conditions, with the maximum 3- to 6-fold induction at approximately 48 to 72 h. *, $P < 0.05$.

Table 2. Survival analysis of JMJD1A

Variable	Univariate analysis	Multivariate analysis	
	P	Relative risk (95% CI)	*P*
Lymph node metastasis (+/–)	<0.0001	6.282 (2.345-16.826)	0.003
Lymphatic invasion (yes/no)	<0.0001	3.535 (1.542-8.10)	0.0029
Duke's classification (CD/AB)	<0.0001		
Depth of invasion (ss~/~mp)	0.0008	1.522 (0.404-5.73)	0.5345
Venous invasion (yes/no)	0.0013	2.25 (1.041-4.86)	0.0392
JMJD1A (high/low)	0.0108	2.891 (1.235-6.43)	0.0139
Tumor site (rectum/colon)	0.264		
Gender (male/female)	0.2762		
Tumor dedifferentiation (moderate/poor/mucinous/well)	0.5574		
Age, y (≥68/<68)	0.9504		

Abbreviations: mp, muscularis propria; ss, subserosa.

Published OnlineFirst September 7, 2010; DOI:10.1158/1078-0432.CCR-10-0407

To find *in vivo* hypoxia-inducible genes, we studied liver metastases from CRC patients. The $CD34^+$ vascular architecture displayed a unique graded decline from the periphery to the central region (Fig. 1B); thus, it was easy to distinguish the region where hypoxic cells were present. We used CA9, which regulates cellular pH and allows cells to survive under hypoxic conditions, as a guide for hypoxic response. The distance from a vessel to the CA9 expression in cancer cells was 80 μm in head and neck tumors, leading to a tissue pO_2 of 1% (36). We also found that CA9 expression was strongly induced in tumor cells positioned approximately 60 to 100 μm from tumor vessels (Fig. 1A, middle), indicating that CA9 was a reliable biomarker for hypoxia in liver metastasis of CRC. In addition, the metastatic cells are thought to originate from a single proliferating cell (37, 38). The homogeneous cell population may be better suited for doing a reliable comparative gene expression study between cells supplied with an abundant flow of blood and those without. By contrast, primary cancer tissue consists of highly heterogeneous cells (39) and oxygen levels are typically heterogeneous within individual tumors (9).

To find novel hypoxia-inducible genes, the method of collecting liver metastasis samples is of particular importance. To avoid surgery-related hypoxia, we consecutively collected only patients who had partial liver resection, but not hepatic lobectomy or segmentectomy; the latter surgery usually requires ligation of the Glissonian branch to reveal a clear ischemic demarcation line on the surface of the liver. Moreover, we stored the liver tissue samples in OCT compound as soon as possible after removal by surgery, usually within 10 to 15 minutes. To assure that our collection method was effective enough to reduce surgery-associated hypoxia to a minimum, we did qRT-PCR before microarray analysis and examined whether well-known hypoxia-associated genes were upregulated in the central region of hepatic metastasis compared with the periphery region. We confirmed that the

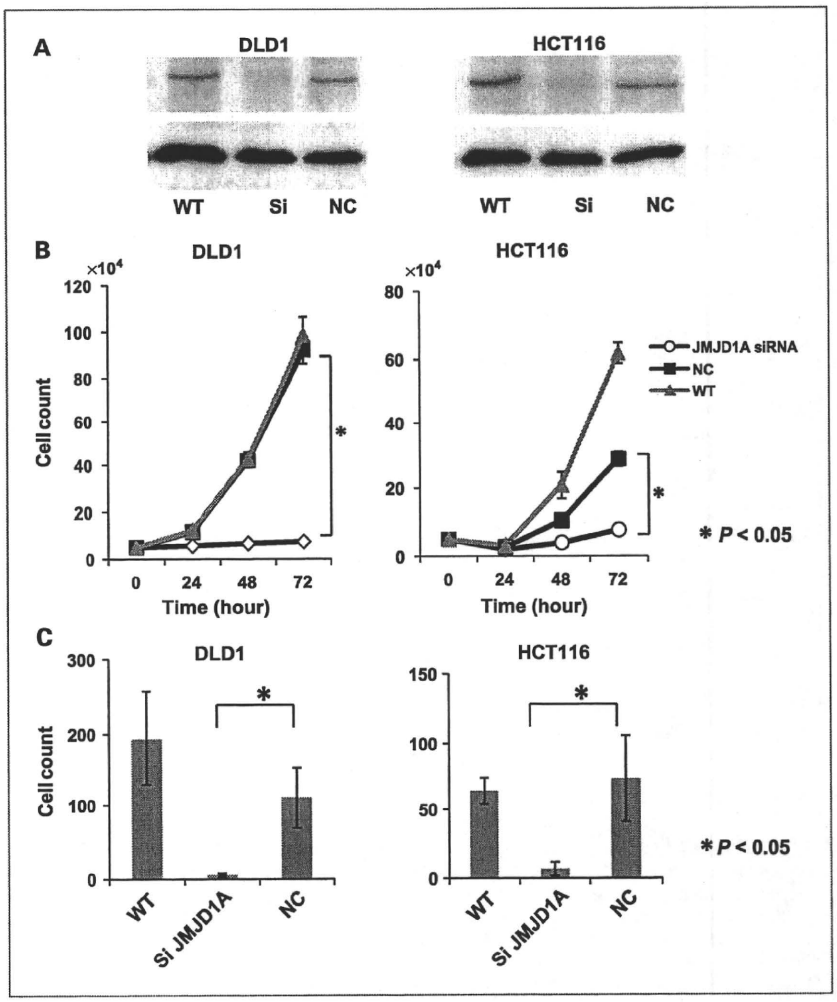

Fig. 3. *In vitro* assessment of JMJD1A expression after knockdown. A, cells were seeded at a density of 1.0×10^5 in six-well dishes in triplicate and counted 24, 48, and 72 h later using a hemocytometer. A significant reduction in JMJD1A by siRNA was noted by Western blotting in DLD1 and HCT116. Actin bands served as loading controls. WT, wild-type. B, cells were seeded at a density of 1.0×10^5 in six-well dishes. Treatment with JMJD1A siRNA displayed significant growth inhibition when compared with the negative control (NC) group in DLD1 and HCT116 ($P < 0.05$ for both). C, invasion assays showed a significant decrease in invaded cell number with treatment of JMJD1A siRNA in DLD1 and HCT116 ($P < 0.05$ for both).

Published OnlineFirst September 7, 2010; DOI:10.1158/1078-0432.CCR-10-0407

angiogenesis-related genes, such as angiopoietin2 (ANG2), VEGF, epidermal growth factor receptor (EGFR), fibroblast growth factor 2 (FGF2), and inducible nitric oxide synthase (iNOS), and the metabolism-related genes, such as GLUT1, GLUT3, lactate dehydrogenase A (LDHA), and phosphoglycerate kinase 1 (PGK1; refs. 1, 10, 40), showed 1.4- to 3.3-fold higher RNA in 12 paired samples (data not shown; primer sequences are shown in Supplementary Table S2). Microarray analysis successfully identified genes highly induced by hypoxia *in vivo*. VEGF ranked 5th among 30,000 human genes; 10 genes among the top 30 were well-known or relatively newly identified hypoxia-inducible genes (Table 1). We further identified several novel hypoxia-inducible gene candidates. The presence of many known hypoxia-related genes and prognostic factors in the list of the top 30 candidate genes is in good compliance with our initial concept that, *in vivo*, hypoxia-related genes should exert rather malignant properties. Because hypoxic stress is involved in cell death and survival, energy preservation, angiogenesis, pH regulation, and glucose metabolism, our data may shed some light on many aspects of cancer biology. After screening the top 30 genes based on a prospective clinical follow-up study in which the primary CRC tissues were analyzed with the same DNA chip, we focused on JMJD1A and concluded by qRT-PCR that JMJD1A is a novel independent prognostic factor for CRC (Table 2).

To assess the prognostic value of JMJD1A, it is important to see its relation to chemotherapy. When we analyzed disease-free survival between a group receiving chemotherapy and one that did not in a prospective series of 214 CRC patients (Supplementary Table S1A), we found that although a tendency was noted ($P = 0.059$), no statistical difference was observed between the two

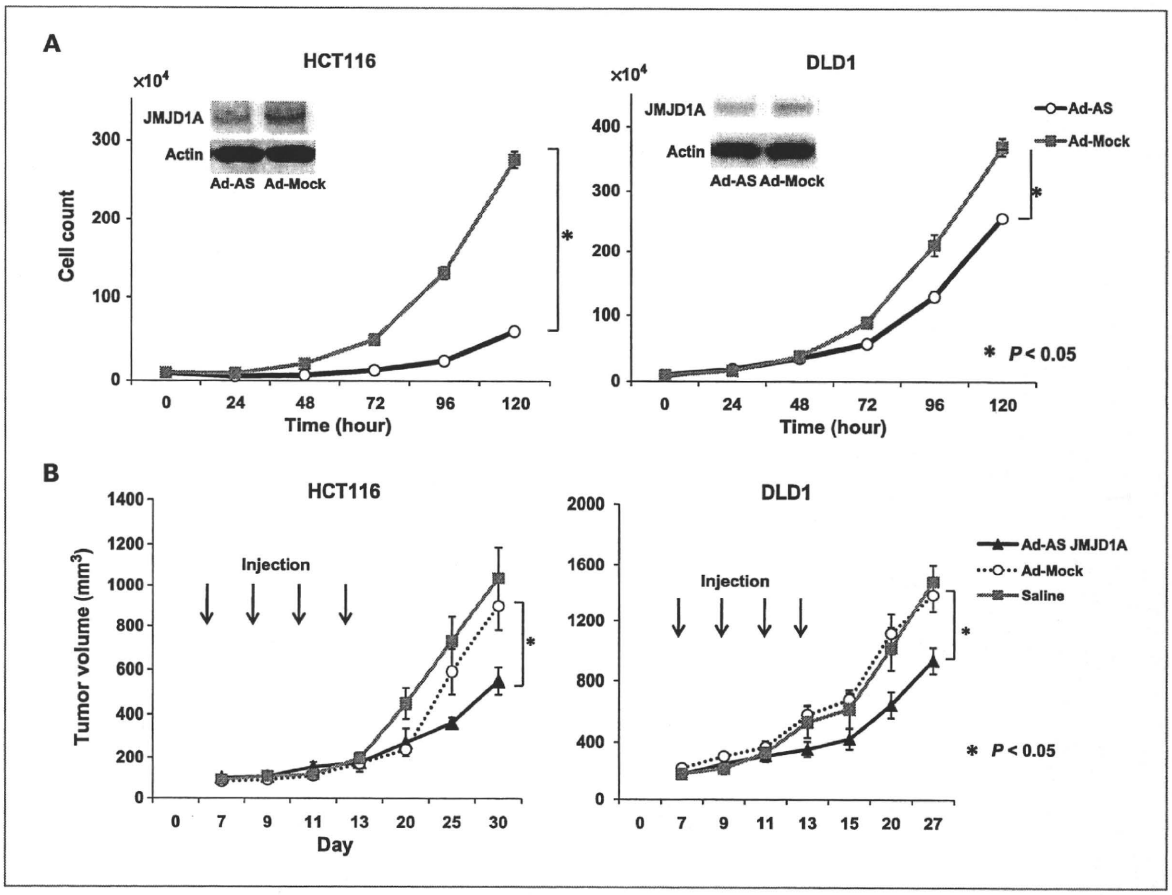

Fig. 4. Effects of Ad-AS JMJD1A on the growth of CRC cells. A, Ad-AS JMJD1A at MOI of 100 significantly inhibited tumor cell growth when compared with the Mock control in DLD1 and HCT116 ($P < 0.05$ for both). Western blot showed that Ad-AS JMJD1A at 100 MOI decreased JMJD1A protein expression at 48 h in DLD1 and HCT116. Actin bands served as loading controls. B, treatment of established tumor xenografts with intratumoral injection of Ad-AS JMJD1A. Subcutaneous xenografts of CRC cells (HCT116 and DLD1) were established in nude mice ($n = 5$ for each group) by injection of 5×10^6 cells. After day 7, Ad-Mock, Ad-AS JMJD1A (1.0×10^9 plaque-forming units per injection), and NaCl solution were injected into tumors and three more injections per tumor were applied on days 9, 11, and 13. Tumor size on day 30 was significantly smaller in the AS group when compared with the Mock control group in both cell types ($P < 0.05$ for both).

Published OnlineFirst September 7, 2010; DOI:10.1158/1078-0432.CCR-10-0407

groups (Supplementary Table S3). However, it was of interest that high expression of JMJD1A was significantly predictive of a poor prognosis in the group receiving chemotherapy ($P = 0.013$), but not in the group that did not receive chemotherapy (data not shown). The findings suggest that JMJD1A may lessen the efficacy of chemotherapy, which is consistent with the concept that hypoxia often makes tumor cells resistant to chemotherapy (8, 9, 35).

Recently, JMJD1A was shown for the first time to be upregulated by hypoxia via HIF-1 (41). Although Wellman et al. observed JMJD1A induction by hypoxia up to 24 hours, our data showed that the JMJD1A expression level continued to increase after 24 hours, reaching a maximum level of induction (3- to 6-fold) at 48 to 72 hours in CRC cell lines. In this regard, our gene list, generated from constitutive *in vivo* expression analysis, may reflect the chronic cellular responses to hypoxia. We also showed by immunohistochemistry that JMJD1A was a sensitive biomarker for *in situ* hypoxic cells (Fig. 2). The expression pattern was consistent with the report that hypoxic tumor cells are generally >100 μm away from functional blood vessels (42).

In vitro mechanistic studies showed that knockdown of JMJD1A reduced tumor cell growth and invasion. We also found that decreased growth effects from JMJD1A inhibition could be observed, irrespective of the VEGF level, in the colon cancer cells through treatment with siRNA against VEGF.[4] Furthermore, the therapeutic *in vivo* models using an adenovirus-mediated antisense strategy against JMJD1A showed that JMJD1A could be a promising therapeutic target in CRC. Epigenetic modifications can affect various characteristics of cancer cells, such as apoptosis, invasion, angiogenesis, and immune recognition (43); therefore, it is possible that JMJD1A has pleiotropic effects in CRC by restoring defective expression of certain genes. We also speculate that JMJD1A might be a universal prognostic factor in human carcinomas via histone modification because our prospective microarray analysis indicated that JMJD1A was associated with poor prognosis in gastric cancer and hepatocellular carcinoma (data not shown). Although many downstream targets should be clarified in the future, a recent study has shown that JMJD1A regulates the expression of ADM and growth and differentiation factor 15 (GDF15) by decreasing histone methylation of these promoters (44). The results are consistent with our findings that both JMJD1A and ADM are novel prognostic markers in CRC.

In conclusion, we showed that JMJD1A could be a sensitive biomarker for hypoxic tumor cells and a poor prognosis of CRC. Our data also suggest that JMJD1A may be a novel therapeutic target, especially against tumor cells in a hypoxic condition.

[4] Unpublished observation.

Disclosure of Potential Conflicts of Interest

There are no potential conflicts of interest in this study.

Acknowledgments

We thank Yurika Nakamura and Ken Konishi for their valuable technical support and Prof. T. Minamoto (Cancer Research Institute, Kanazawa, Japan) for providing the KM12SM colon cancer cell line.

Grant Support

3rd-term Comprehensive Strategy for Cancer Control from the Ministry of Health, Labour, and Welfare; Grant-in-Aid for Cancer Research from the Ministry of Education, Science, Sports, and Culture, Japan; and Sagawa Foundation for Promotion of Cancer Research.

The costs of publication of this article were defrayed in part by the payment of page charges. This article must therefore be hereby marked *advertisement* in accordance with 18 U.S.C. Section 1734 solely to indicate this fact.

Received 02/15/2010; revised 07/12/2010; accepted 07/13/2010; published OnlineFirst 09/07/2010.

References

1. Semenza GL. Hypoxia and cancer. Cancer Metastasis Rev 2007;26:223–4.
2. Colpaert C, Vermeulen P, van Beest P, et al. Intratumoral hypoxia resulting in the presence of a fibrotic focus is an independent predictor of early distant relapse in lymph node-negative breast cancer patients. Histopathology 2001;39:416–25.
3. Koukourakis MI, Giatromanolaki A, Sivridis E, et al. Hypoxia-regulated carbonic anhydrase-9 (CA9) relates to poor vascularization and resistance of squamous cell head and neck cancer to chemoradiotherapy. Clin Cancer Res 2001;7:3399–403.
4. Giatromanolaki A, Koukourakis MI, Sivridis E, et al. Expression of hypoxia-inducible carbonic anhydrase-9 relates to angiogenic pathways and independently to poor outcome in non-small cell lung cancer. Cancer Res 2001;61:7992–8.
5. Fyles A, Milosevic M, Hedley D, et al. Tumor hypoxia has independent predictor impact only in patients with node-negative cervix cancer. J Clin Oncol 2002;20:680–7.
6. Vaupel P, Mayer A. Hypoxia in cancer: significance and impact on clinical outcome. Cancer Metastasis Rev 2007;26:225–39.
7. Chi JT, Wang Z, Nuyten DS, et al. Gene expression programs in response to hypoxia: cell type specificity and prognostic significance in human cancers. PLoS Med 2006;3:e47.
8. Harris AL. Hypoxia—a key regulatory factor in tumour growth. Nat Rev Cancer 2002;2:38–47.
9. Kizaka-Kondoh S, Inoue M, Harada H, Hiraoka M. Tumor hypoxia: a target for selective cancer therapy. Cancer Sci 2003;94:1021–8.
10. Semenza GL. Targeting HIF-1 for cancer therapy. Nat Rev Cancer 2003;3:721–32.
11. Hurwitz H, Fehrenbacher L, Novotny W, et al. Bevacizumab plus irinotecan, fluorouracil, and leucovorin for metastatic colorectal cancer. N Engl J Med 2004;350:2335–42.
12. Arun C, London NJ, Hemingway DM. Prognostic significance of elevated endothelin-1 levels in patients with colorectal cancer. Int J Biol Markers 2004;19:32–7.
13. Okada Y, Scott G, Ray MK, Mishina Y, Zhang Y. Histone demethylase JHDM2A is critical for Tnp1 and Prm1 transcription and spermatogenesis. Nature 2007;450:119–23.
14. Yamane K, Toumazou C, Tsukada Y, et al. JHDM2A, a JmjC-containing H3K9 demethylase, facilitates transcription activation by androgen receptor. Cell 2006;125:483–95.

Published OnlineFirst September 7, 2010; DOI:10.1158/1078-0432.CCR-10-0407

15. McShane LM, Altman DG, Sauerbrei W, Taube SE, Gion M, Clark GM. REporting recommendations for tumor MARKer prognostic studies (REMARK). Nat Clin Pract Oncol 2005;2:416–22.
16. Hayashi N, Yamamoto H, Hiraoka N, et al. Differential expression of cyclooxygenase-2 (COX-2) in human bile duct epithelial cells and bile duct neoplasm. Hepatology 2001;34:638–50.
17. Ogawa M, Yamamoto H, Nagano H, et al. Hepatic expression of ANG2 RNA in metastatic colorectal cancer. Hepatology 2004;39: 528–39.
18. Yamamoto H, Kondo M, Nakamori S, et al. JTE-522, a cyclooxygenase-2 inhibitor, is an effective chemopreventive agent against rat experimental liver fibrosis. Gastroenterology 2003;125:556–71.
19. Takeno A, Takemasa I, Doki Y, et al. Integrative approach for differentially overexpressed genes in gastric cancer by combining large-scale gene expression profiling and network analysis. Br J Cancer 2008;99:1307–15.
20. Nagel S, Schmidt M, Thiede C, Huhn D, Neubauer A. Quantification of Bcr-Abl transcripts in chronic myelogenous leukemia (CML) using standardized, internally controlled, competitive differential PCR (CD-PCR). Nucleic Acids Res 1996;24:4102–3.
21. Hoshino H, Miyoshi N, Nagai K, et al. Epithelial-mesenchymal transition with expression of SNAI1-induced chemoresistance in colorectal cancer. Biochem Biophys Res Commun 2009;390: 1061–5.
22. Yasui M, Yamamoto H, Ngan CY, et al. Antisense to cyclin D1 inhibits vascular endothelial growth factor-stimulated growth of vascular endothelial cells: implication of tumor vascularization. Clin Cancer Res 2006;12:4720–9.
23. Ishigami SI, Arii S, Furutani M, et al. Predictive value of vascular endothelial growth factor (VEGF) in metastasis and prognosis of human colorectal cancer. Br J Cancer 1998;78:1379–84.
24. Arun C, DeCatris M, Hemingway DM, London NJ, O'Byrne KJ. Endothelin-1 is a novel prognostic factor in non-small cell lung cancer. Int J Biol Markers 2004;19:262–7.
25. Boldrini L, Gisfredi S, Ursino S, et al. Expression of endothelin-1 is related to poor prognosis in non-small cell lung carcinoma. Eur J Cancer 2005;41:2828–35.
26. Wulfing P, Diallo R, Kersting C, et al. Expression of endothelin-1, endothelin-A, endothelin-B receptor in human breast cancer and correlation with long-term follow-up. Clin Cancer Res 2003;9: 4125–31.
27. Couvelard A, Deschamps L, Rebours V, et al. Overexpression of the oxygen sensors PHD-1, PHD-2, PHD-3, and FIH is associated with tumor aggressiveness in pancreatic endocrine tumors. Clin Cancer Res 2008;14:6634–9.
28. Yamachika T, Werther JL, Bodian C, et al. Intestinal trefoil factor: a marker of poor prognosis in gastric carcinoma. Clin Cancer Res 2002;8:1092–9.
29. Dhar DK, Wang TC, Tabara H, et al. Expression of trefoil factor family members correlates with patient prognosis and neoangiogenesis. Clin Cancer Res 2005;11:6472–8.
30. Hata K, Takebayashi Y, Akiba S, et al. Expression of the adrenomedullin gene in epithelial ovarian cancer. Mol Hum Reprod 2000;6: 867–72.
31. Yamazaki T, Kanda T, Sakai Y, Hatakeyama K. Liver fatty acid-binding protein is a new prognostic factor for hepatic resection of colorectal cancer metastases. J Surg Oncol 1999;72:83–7.
32. Jiang Y, Zou L, Zhang C, et al. PPARγ and Wnt/β-catenin pathway in human breast cancer: expression pattern, molecular interaction and clinical/prognostic correlations. J Cancer Res Clin Oncol 2009;135: 1551–9.
33. Hoog C, Schalling M, Grunder-Brundell E, Daneholt B. Analysis of a murine male germ cell-specific transcript that encodes a putative zinc finger protein. Mol Reprod Dev 1991;30:173–81.
34. Loh YH, Zhang W, Chen X, George J, Ng HH. Jmjd1a and Jmjd2c histone H3 Lys 9 demethylases regulate self-renewal in embryonic stem cells. Genes Dev 2007;21:2545–57.
35. Brennan DJ, Jirstrom K, Kronblad A, et al. CA IX is an independent prognostic marker in premenopausal breast cancer patients with one to three positive lymph nodes and a putative marker of radiation resistance. Clin Cancer Res 2006;12:6421–31.
36. Beasley NJ, Wykoff CC, Watson PH, et al. Carbonic anhydrase IX, an endogenous hypoxia marker, expression in head and neck squamous cell carcinoma and its relationship to hypoxia, necrosis, and microvessel density. Cancer Res 2001;61:5262–7.
37. Fidler IJ. Selection of successive tumour lines for metastasis. Nat New Biol 1973;242:148–9.
38. Fidler IJ. The pathogenesis of cancer metastasis: the 'seed and soil' hypothesis revisited. Nat Rev Cancer 2003;3:453–8.
39. Korn WM, Yasutake T, Kuo WL, et al. Chromosome arm 20q gains and other genomic alterations in colorectal cancer metastatic to liver, as analyzed by comparative genomic hybridization and fluorescence *in situ* hybridization. Genes Chromosomes Cancer 1999;25:82–90.
40. Liao D, Johnson RS. Hypoxia: a key regulator of angiogenesis in cancer. Cancer Metastasis Rev 2007;26:281–90.
41. Wellmann S, Bettkober M, Zelmer A, et al. Hypoxia upregulates the histone demethylase JMJD1A via HIF-1. Biochem Biophys Res Commun 2008;372:892–7.
42. Helmlinger G, Yuan F, Dellian M, Jain RK. Interstitial pH and pO_2 gradients in solid tumors *in vivo*: high-resolution measurements reveal a lack of correlation. Nat Med 1997;3:177–82.
43. Sigalotti L, Fratta E, Coral S, et al. Epigenetic drugs as pleiotropic agents in cancer treatment: biomolecular aspects and clinical applications. J Cell Physiol 2007;212:330–44.
44. Krieg AJ, Rankin EB, Chan D, Razorenova O, Fernandez S, Giaccia AJ. Regulation of the histone demethylase JMJD1A by HIF-1α enhances hypoxic gene expression and tumor growth. Mol Cell Biol 2009;30: 344–53.

Journal of Surgical Oncology 2010;101:376–383

Multidetector Computed Tomography for Preoperative Prediction of Postsurgical Prognosis of Patients with Extrahepatic Biliary Cancer

SHOGO KOBAYASHI, MD, PhD,[1] HIROAKI NAGANO, MD, PhD,[1]* SHIGERU MARUBASHI, MD, PhD,[1] HIROSHI WADA, MD, PhD,[1] HIDETOSHI EGUCHI, MD, PhD,[1] YUTAKA TAKEDA, MD, PhD,[1] MASAHIRO TANEMURA, MD, PhD,[1] TONSOK KIM, MD, PhD,[2] YUICHIRO DOKI, MD, PhD,[1] AND MASAKI MORI, MD, PhD[1]

[1]*Department of Surgery, Osaka University, Yamadaoka 2-2(E2), Suita, Osaka, Japan*
[2]*Department of Surgery and Radiology, Osaka University, Yamadaoka 2-2(E2), Suita, Osaka, Japan*

Background: Preoperative prognostic information to select a treatment strategy is important especially in patients who need highly aggressive surgery, such as those with biliary cancer. We evaluated various prognostic factors and non-curative surgical factors using multidetector computed tomography (MDCT).

Methods: We retrospectively analyzed 71 patients who underwent MDCT preoperatively and were scheduled for surgical resection of biliary cancer. For MDCT diagnosis, we used MDCT-based classification equivalent to the surgical and pathological classification of the Japanese Society of Biliary Surgery. We evaluated MDCT-related prognostic factors and non-curative surgical factors and compared these factors with pathological results.

Results: MDCT-diagnosed category T (primary tumor invasion) included both prognostic factors and non-curative surgical factors but not category N (lymph node metastasis). Multivariate analysis identified MDCT-based suspected arterial invasion as an independent prognostic factor. In patients suspected of arterial invasion by MDCT, the 3-year overall survival rate was only 39% and the curative resection ratio was only 33%, because of the high positive surgical dissected margin.

Conclusion: MDCT-based suspected arterial invasion is a predictor of poor prognosis after surgery for biliary cancer and represents a non-curative surgical factor associated with positive dissected margin.

J. Surg. Oncol. 2010;101:376–383. © 2010 Wiley-Liss, Inc.

KEY WORDS: **biliary cancer; surgery; MDCT**

INTRODUCTION

At present, complete resection is one of the most effective treatments for local extrahepatic biliary cancer. The indication and selected type of surgery are based on the results of various imaging studies; however, the rate of curative resection according to the Japanese Society of Biliary Surgery (JSBS) has not exceeded 80% [1,2]. On the other hand, the development of multidetector computed tomography (MDCT) allowed establishing accurate diagnosis, especially in vertical extension [3], that is, invasion of the hepatic artery or portal vein. Okumoto et al. [4] reported the relationship between CT images of biliary tract tumors and histopathological invasion.

The resection procedure for biliary cancer is often aggressive. Therefore, understanding the preoperative factors that influence prognosis and curative resection might help in the selection of appropriate surgical strategy and avoid unnecessary surgery, which could ultimately improve prognosis. Based on the above reasons, we evaluated the prognostic factors in MDCT-based preoperative diagnosis in patients who were planned for curative resection. For the evaluation, we established criteria for MDCT-based diagnosis based on the surgical criteria of JSBS [1], which were also closely related to the CT-based diagnostic criteria recommended by Okumoto et al. [4]. This approach stemmed from the lack of appropriate criteria for MDCT-diagnosis that correlate with the surgical and pathological classifications. Analysis of preoperative MDCT data could provide a better prediction of prognosis, to select appropriate treatment, including surgery and neoadjuvant therapy.

Previous studies reported the relationship between diagnosis by MDCT and pathological diagnosis [4–13] in about 20 patients; however, there was no data for the respectability and/or the prognosis related to MDCT diagnosis. Recently, another strategy for biliary cancer, other than surgery, for example, chemotherapy with or without irradiation, has been tested. Information on the curative resection rate and prognosis of patients scheduled for surgery are important for any decision on treatment strategies. In the present study, we evaluated the prognostic and non-curative surgical factors among MDCT-related factors in cases planned for surgery.

Abbreviations: CEA, carcino-embryonic antigen; CTC, circulating tumor cells; fCur, final curability; FDG–PET, F-fluorodeoxyglucose–positron emission tomography; fStage, final stage; JSBS, Japanese Society of Biliary Surgery; MDCT, multidetector computed tomography; MRI, magnetic resonance imaging; OS, overall survival rate; PTPE, percutaneous transhepatic portal vein embolization; qPCR; quantitative polymerase chain reaction; SUV, standardized uptake values.

Contribution of Each Author: "designed research/study" Hiroaki Nagano, Yuichiro Doki, Masaki Mori, "performed research/study" Shogo Kobayashi, Shigeru Marubashi, "contributed important reagents" none, "collected data" Hidetoshi Eguchi, Yutaka Takeda, Masahiro Tanemura, "analyzed data" Shogo Kobayashi, "wrote the paper " Shogo Kobayashi, Hiroaki Nagano.

*Correspondence to: Hiroaki Nagano, MD, PhD, Department of Surgery, Graduate School of Medicine, Osaka University, Yamadaoka 2-2(E2), Suita, Osaka 565-0871, Japan. Fax: +81-6-6879-3259.
E-mail: hnagano@gesurg.med.osaka-u.ac.jp

Received 29 September 2009; Accepted 17 December 2009

DOI 10.1002/jso.21501

Published online 8 March 2010 in Wiley InterScience (www.interscience.wiley.com).

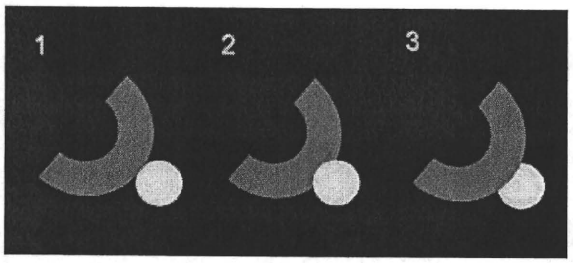

Fig. 1. Schematic diagram of MDCT-based diagnosis of invasion in biliary cancer. Gray open circle: biliary duct with cancer, white closed circle: enhanced vessels by contrast media. (1) Doubtful invasion: suspected cancer of the biliary duct attached to the vessel at a single point without space. (2) Definite invasion: suspected cancer of the biliary duct widely attached to the vessel; the latter shows no narrowing. (3) Severe invasion: suspected cancer of the biliary duct apparently invading the vessel and the vessel shows narrowing or obstruction.

PATIENTS AND METHODS

MDCT Criteria for Diagnosis and Rules for Classification of Cholangiocarcinoma

In this study, we used JSBS general rules for classification of biliary cancer: Surgical and Pathological Studies on Cancer of the Biliary Tract (5th edition) [1] to establish our criteria for MDCT diagnosis (Figure 1 and Table IA). These criteria were closely related to the CT diagnostic criteria of Okumoto et al. [4] for vascular invasion. The schematic diagram in the Figure 2 illustrates our classification of invasion and comparison with JSBS classification for surgery and pathology as well as the CT classification used by Okumoto et al. [4]. As example, we showed JSBS classification of extrahepatic bile duct cancer in Table IB.

Patients

We retrospectively analyzed all 71 patients who underwent MDCT preoperatively and who were scheduled for surgical resection up to 2007 at our institution. Table II shows the clinicopathological features of these patients. The median follow-up period was 18.4 months

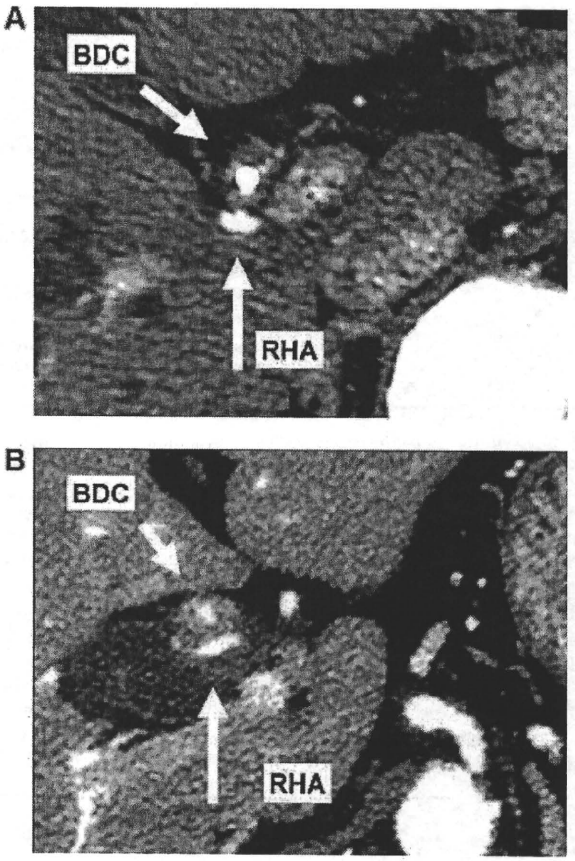

Fig. 2. Representative figure of CT-A. The figure showed the tumor (BDC) closely attached to the right hepatic artery (RHA). **A**: CT-A1, **B**: CT-A2.

(range, 0.3–96.7), and during this follow-up period 27 (38.0%) patients died. All patients received regular follow-up with abdominal CT and measurement of serum carcinoembryonic antigen (CEA) every 3 months in the first 2 years and every 6 months later after

TABLE IA. Diagnostic Criteria for Preoperative MDCT, Based on JSBS Surgical Criteria

JSBS classification	Our MDCT criteria	CT criteria of Okumoto et al. [4]
Invasion of the hepatic artery (A) or portal vein (PV)		
0: No invasion		0
1: Doubtful invasion	Main tumor attached to the vessel	1a
2: Definite invasion	Between 1 and 3	1b, 2
3: Severe invasion (narrowing or obstruction)	Main tumor clearly invading the vessel	3, 4
Invasion of the liver (Hinf), biliary duct (Binf), and gall bladder (Ginf), pancreas (Panc)		
0: No invasion		
1: Doubtful invasion	Main tumor attached to the liver	
2: Definite invasion, but around the primary tumor	Main tumor clearly invading the liver	
3: Severe invasion but around the primary tumor	Main tumor severely invading the liver	
Invasion of the serosa		
0: No invasion		
1: Doubtful invasion	Main tumor attached to the serosa	
2: Definite invasion	Between 1 and 3	
3: Invasion of other organs	Main tumor invading other organs	
Lymph node metastasis		
0: No evidence of lymph node metastasis	Major axis <1 cm	
1: Lymph node metastasis	Major axis ≥ 1 cm	

TABLE IB. JSBS Classification in Extrahepatic Bile Duct Cancer

T category (pathological T category (pT)), primary tumor invasion					
(p)T1	S0 (m, fm)	(p)Hinf0	(p)Panc0	(p)PV0	(p)A0
(p)T2	S1 (ss)	Hinf1 (pHinf1a)	Panc1(pPanc1a)	(p)PV0	(p)A0
(p)T3	S2,3 (se)	Hinf1 (pHinf1b)	Panc1(pPanc1b)	(p)PV0	(p)A0
(p)T4	Any (any)	(p)Hinf 2,3	(p)Panc 2,3	(p)PV 1,2,3	(p)A 1,2,3

S, Hinf, Panc, PV, A were abbreviated at table 1A.

N category (lymph node metastasis groups)

N1: lymph node around the extrahepatic biliary duct.

N2: lymph node in the hepatoduodenal ligament, around common hepatic artery, and around superior retropancreas.

N3: the other lymph node around pancreas than N1 and N2, lymph node around celiac artery, and paraaortic lymph node.

Surgical stage (sStage) and final stage (fStage)

	H0, P0, M(-)				H1,2,3 P1,2,3, M(+)
	(p)N0	(p)N1	(p)N2	(p)N3	
(p)T1	I	II		IVa	IVb
(p)T2	II	III			
(p)T3			IVa		
(p)T4	IVa				

Final curability (fCur)

	H	P	pN-D	pDM	pHM	pEM	M
fCur A	H0	P0	pN<D	pDM0	pHM0	pEM0	M(-)
fCur B	Other than fCur A and fCur C						
fCur C	H1,2,3	P1,2,3	pN>D	pDM2	pHM2	pEM2	M(+)

H0 = no evidence of liver metastasis; H1 = metastasis limited to one lobe; H2 = a few metastases to both lobes; H3 = numerous metastases to both lobes; P0 = no evidence of peritoneal metastasis; P1 = metastasis to the peritoneum adjacent to extrahepatic bile ducts; P2 = a few metastases to the distant peritoneum; P3 = numerous metastases to the distant peritoneum; M = distant metastasis other than peritoneal and/or liver metastases; pN = histological lymph node metastasis; D = lymph node dissection; pDM = distal (duodenal) cut end; pHM = proximal (hepatic) cut end; pEM = dissected periductal structure; pDM0, pHM0, pEM0 = cancer-free margin of more than 5 mm in width; pDM1, pHM1, pEM1 = cancer-free margin of 5 mm or less in width; pDM2, pHM2, pEM2 = definite invasion of each surgical margin.

surgery. Eight (11.3%) received adjuvant therapy (five chemotherapy that included two on gemcitabine and three radiotherapy). Recurrence developed in 27 (38.0%) patients and 13 were treated with gemcitabine, while 2 received radiotherapy.

MDCT Imaging

MDCT was performed either with a LightSpeed Qxi scanner (GE Medical Systems, Waukesha, WI), a LightSpeed VCT scanner (GE Medical Systems) or with an Aquilion 64 scanner (Toshiba Medical Systems, Tokyo, Japan) using a tube voltage of 120 kV, a tube current of 300 mA, and a rotation time of 0.5 sec. Images of at least 0.625-mm slice thickness were used for evaluation. Contrast-enhanced multiphasic CT images were acquired at 10 sec after the peak aortic enhancement (arterial phase), followed by the portal venous phase and hepatic venous phase for the upper abdomen. Non-ionic contrast medium (300 mg/ml iodine) was administered intravenously at a rate of 2–4 ml/sec using a power injector.

CT-Based Staging

All CT images were used for staging. At least two radiologists or surgeons staged the disease preoperatively, according to the above classification, using preoperative MDCT. Trans-ampullary biliary drainage was performed in 22 (31.0%) patients during MDCT. We evaluated the invasion of the primary tumor into the hepatic artery (CT-A), portal vein (CT-PV), serosa (CT-S), and adjacent organs (liver, gall bladder from the bile duct, bile duct from the gall bladder,

TABLE II. Clinicopathological Features of Participating Patients and Their Survival Rate

	N	3-year overall survival rate (%)	P
Age (years)			
≥65	43	48	0.3541
<65	28	64	
Sex			
Male	43	48	0.3402
Female	28	67	
Diagnosis			
Extrahepatic bile duct	40	50	0.3885
Gall bladder	22	54	
Ampulla of Vater	9	76	
pT			
1/2/3	29	71	0.0009
4	29	35	
pN			
0/1	41	59	0.0853
2/3	24	42	
fStage			
1/2/3	23	78	0.0006
4a/b	35	6	
fCur			
A/B	49	63	0.0105
C	22	32	

and pancreas) and decided on the T category (CT-T) using JSBS classification for surgery. After evaluation of lymph node metastasis by MDCT (major axis ≥1 cm was considered positive, CT-N) we judged the CT-based stage (CT-stage).

Pathological Diagnosis

Pathological diagnosis was based on JSBS classification. For histopathological examination, 6-μm paraffin-embedded sections were prepared for each 5-mm serial section along the axial length of the biliary tract. The pathological diagnosis was compared retrospectively with CT-based diagnosis. For example, pathological invasion of the hepatic artery was abbreviated as pA, and pA1, pA2, pA3 indicated invasion of the adventitia, media, intima, and/or lumen of the hepatic artery, respectively.

Statistical Analysis

Overall survival (OS) rates were calculated by the Kaplan–Meier method and differences in CT-diagnosis factors were tested by the log-rank test. Differences in the curative resection ratio and the relationship between CT-N and pathological lymph node metastasis were analyzed by the Student's *t*-test or chi-square test. Multivariate analysis was performed using Cox proportional-hazards regression model. A P value of <0.05 was considered statistically significant. The statistical software used was StatView J-5.0 software (SAS, Cary, NC).

RESULTS

Patients Survival Rate According to Pathological Diagnosis

Table II also shows patients survival according to pathological diagnosis. The OS rate at 3 years was 54.3%. The curative resection ratio (fCurA and B) was 69%. The pathological prognostic factors were T category (pT), final stage (fStage), and final curability (fCur) similar to other patients with biliary cancer, except for a trend in pathological lymph node metastasis (pN, $P = 0.0853$).

Overall Survival Rate According to MDCT-Based Diagnosis

Based on the above classification for preoperative MDCT-diagnosis, CT-staging was performed and the CT-stage-dependent survival was calculated (Table III). There was a significant difference

TABLE III. MDCT Staging and Prognosis

			Univariate	Multivariate		
	n	3-year overall survival rate (%)	P	Hazard ratio	95% CI	P
CT-T						
T1/2/3	33	75	0.0050			
T4	38	36				
CT-N						
N0/1	48	63	0.6052			
N2/3	23	43				
CT-Stage						
Stage 1/2	26	79	0.0649			
Stage 3/4a	30	51				
Stage 4b	15	26				
CT-A						
A0	41	67	0.0163	2.625	1.176–5.848	0.0184
A1/2/3	30	39				
CT-PV						
PV0	51	56	0.4082			
PV1/2/3	20	51				
CT-S						
S0	10	62	0.2350			
S1	29	49				
S2/3	10	23				
CT-Hinf/Ginf/Binf/Panc						
0	47	62	0.0492	2.077	0.966–4.467	0.0614
1	9	56				
2/3	15	28				

TABLE IV. MDCT Staging Rate for fCurA/B Resection

	n	fCurA/B	Rate (%)	P
CT-T				
1/2/3	33	28	85	0.0072
4	38	21	55	
CT-N				
0	44	33	75	0.2701
1	4	2	50	
2	16	9	56	
CT-Stage				
1/2	26	22	85	<0.0001
3/4a	30	20	67	
4b	8	0	0	
CT-A				
0	41	35	85	0.0017
1	24	12	50	
2/3	6	2	33	
CT-P				
0	51	39	76	0.0836
1	13	6	46	
2/3	7	4	57	
CT-S				
0	10	9	90	0.0594
1	29	16	55	
2/3	10	4	40	
CT-Hinf/Ginf/Binf/Panc				
0	47	34	72	0.6583
1	9	6	67	
2/3	15	9	60	

in OS rate between CT-T 1/2/3 and CT-T 4 (3-year OS rates: 75% and 36%, respectively, $P=0.0050$). However, there was no significant difference in OS rate based on CT-N. For category T, CT-A and invasion of adjacent organs correlated with prognosis, and multivariate analysis identified CT-A as the only independent factor related to prognosis (hazard ratio = 2.625, $P=0.184$). The 3-year OS rate of patient with CT-A (CT-A 1/2/3) was 39%.

Curative Resection Rate in MDCT-Based Diagnosis

We also calculated the curative resection rate (rate of fCur A and B in JSBS classification) (Table IV). fCur A or B is defined as pathologically negative margin and wider lymph node dissection than pathological metastasis; in other words, R0 resection. CT-T correlated significantly with the curative resection ratio ($P=0.0072$). The curative resection rate for CT-T4 was only 55%. For category T, curative resection correlated with only CT-A, and the curative resection rate for CT-A 2/3 was 33% ($P=0.0017$).

We also analyzed the reasons for non-curative resection (fCur C, Table V). The major reason for non-curative resection in patients with CT-A0 was lymph node metastasis. In contrast, approximately 70% of patients with CT-A 1/2/3 have pathologically positive surgical margin and 45% of these patients had a positively dissected margin (Table V).

Relationship Between MDCT-Based Diagnosis and Pathological Diagnosis

We compared the relationship between MDCT-based diagnosis and pathological diagnosis based on JSBS classification for histopathological findings. To estimate lymph node metastasis (N category), we used the lymph node metastasis groups (Table VI). Twenty-four of 65 (37%) were diagnosed as CT-N-positive, while 31 (48%) were pathologically positive. However, there was no relationship between CT-N and pathological N (pathological lymph node metastasis, $P=0.6631$, Table VI).

On the other hand, in T category, we compared CT-A factor (hepatic artery invasion), which correlated with OS and the curative resection ratio, with pathological diagnosis (pA, Tables VII and VIII). For factor A calculated for the whole biliary cancer (bile duct, gall bladder, and ampulla cancer), CT-A was positive (CT-A 1/2/3) in 12 patients among 41 fCur A/B patients (29%), whereas pathological A (pA) was positive in only a single CT-A1 patient. One patient classified as CT-A3 (ipsilateral artery of the resected liver) had no pathological invasion of the hepatic artery. On the other hand, in fCur C patients, 13 of 16 patients (81%) were CT-A positive (CT-A1/2/3), and 2 of these patients were classified pathologically to have arterial invasion (pA2). Three of these patients were CT-A2 or CT-A3 of ipsilateral artery of the resected liver; however, they were negative for pathological arterial invasion.

Furthermore, for hilar biliary cancer, hepatic artery invasion was more closely related to curative resection. We also analyzed the correlation between liver resection with contralateral hepatic artery resection and pathological diagnosis (Table VIII). The contralateral hepatic artery resection was performed in two patients and their pathological diagnosis for contralateral hepatic artery invasion was negative. Invasion of the hepatic artery was diagnosed pathologically in two of CT-A1 patients and these were ipsilateral hepatic artery of the resected liver. The pathological positive rate was 11% (2/18).

DISCUSSION

In this study, we evaluated MDCT-based prognostic factors using surgical and pathological classification-related criteria. For discussion of MDCT diagnosis, one should separately evaluate the three different components of tumor factors in biliary cancer: vertical extension (T category), horizontal extension, and lymph node metastasis (N category). We herein discuss CT-staging related factors: T and N category, excluding horizontal extension.

For the T category, CT-A 1/2/3 was both a prognostic factor and non-curative surgical factor. This factor did not correlate with pathological arterial invasion but was dissected margin-positive. Previous studies have not provided clear definition criteria for CT diagnosis of vascular invasion. Only Okumoto et al. [4] reported the relationship between MDCT and pathological diagnosis, and their criteria 1b (our CT-A2/3) correlated with pathological invasion of the right hepatic artery. In our study, only six cases were classified as CT-A2 (Okumoto's 1b) and the data on these patients could not define a clear relationship with the pathological diagnosis. On the other hand, 24 cases were diagnosed as CT-A1 and histopathological examination

TABLE V. Reasons for fCurC in MDCT-A Status

CT-A	n	fCurC (%)	Margin (+)[a]	Dissected margin (+)[b]
0	41	6 (15%)	0/6 (0%)	—
1/2/3	30	16 (53%)	11/16 (69%)	5/11 (45%)

[a]Pathologically positive surgical margin at hepatic, duodenal, or dissected periductal structures.
[b]Pathologically positive surgical margin at dissected periductal structures at least.

TABLE VI. Lymph Node Metastasis of MDCT Staging and Pathological Diagnosis

CT-N	pN0	pN1	pN2	pN3	pN1/2/3	Total
CT-N0	23	5	7	6	18	41
CT-N1	3	0	1	0	1	4
CT-N2	5	1	5	4	10	15
CT-N3	3	1	1	0	2	5
CT-N1/2/3	11	2	7	4	13	24
Total	34	7	14	10	31	65

$P = 0.6631$.

of these patients was negative for arterial invasion, but showed a high positive rate of dissected margin. It should be noted that MDCT was performed with at least an interval of 0.625 mm, and the slides of the fixed specimen for pathological diagnosis should be at an interval of 5 mm for each. It is possible that pathological diagnosis underestimates arterial invasion because of the 5-mm interval. Furthermore, MDCT showed only intraluminal space of the vessels and it is difficult to discuss the relationship between the tumor and the vessel wall itself in CT. This methodological limitation may also impact the high positive rate of the dissected margin and this should lead to poor prognosis in CT-A 1/2/3 patients. Thus, fCur A/B (R0) resection and the touch smear cytology [14] might be useful for accurate diagnosis and decision on arterial resection.

The next question about arterial invasion is prognosis of patients with pathologically positive tumors for arterial invasion (pA (+)). In this study, only one patient was positive for pathological arterial invasion after fCur A/B (R0) resection, and thus we could not evaluate prognosis according to pathological arterial invasion.

On the other hand, the other factors of T category (CT-PV and CT-S), with the exception of CT-Hinf/Ginf/Binf/Panc, did not correlate with prognosis and curative resection. CT-Hinf/Ginf/Binf/Panc was identified as a prognostic factor in univariate analysis and showed marginal statistical significance in multivariate analysis, although it did not correlate with curative resection. Thus, this factor is a potentially suitable prognostic factor but not non-curative surgery factor, although further studies of larger population samples are needed to confirm these results.

For the N category, CT-N was neither a prognostic factor nor a non-curative surgical factor. Previous reports indicated that the detection of pathological metastasis to lymph node is difficult with a sensitivity of approximately 50% [6–10]. In our study, there was no relationship between MDCT-based diagnosis and pathological metastasis. The CT-criteria used for lymph node metastasis differed slightly among various groups; however, the sensitivity was low in each study. MDCT could not detect lymph node metastasis and therefore could not rule out lymph node metastasis-related non-curative (fCurC, R2) resection based on the diagnostic criteria. Another imaging modality, the F-fluorodeoxyglucose–positron emission tomography (FDG–PET) and/or magnetic resonance imaging (MRI), provides a better detection of pathological lymph node metastasis; however, the sensitivity of the diagnosis using FDG–PET is still low (~50%) under unclear cut-off information of standardized uptake values (SUV)max [15–17], and the diagnosis of lymph node metastasis in biliary cancer by MRI has rarely been reported. Based on this background, preoperative detection of lymph node metastasis in biliary cancer is limited even by the most advanced imaging modalities. To avoid fCur C (non-curative; R2) resection based on lymph node or other distant metastasis, we should develop new diagnostic criteria or modality; for example, methionine PET [18] or circulating tumor cells (CTC) [19–22]. Especially for CTC, we reported recently that CEA estimated by quantitative polymerase chain reaction (qPCR) is a good marker for the detection of micrometastasis [19]. In this regard, CTC is used in hepatocellular carcinoma to predict recurrence and poor prognosis [19–22]. Further studies are needed to determine whether circulating CEA-positive cells in biliary cancer could be used to predict regional and/or distant metastasis.

Using MDCT, our study detected preoperative prognostic factors and non-curative surgery factors, including arterial invasion. This factor relates to local extension but not to regional metastasis (e.g., regional lymph node metastasis). This result would be helpful in deciding the eligibility criteria for neoadjuvant therapy. Recent studies described new regimens of anti-cancer drugs for biliary cancer, including gemcitabine with cisplatin, oxaliplatin, and capecitabine [23–27]. Furthermore, recent clinical trials of chemoradiotherapy for unresectable locally advanced biliary cancer have been reported [28–30]. Perhaps, the next treatment strategy would include neoadjuvant chemoradiotherapy similar to that available for locally advanced pancreatic cancer with suspected arterial and/or portal

TABLE VII. MDCT-Evaluated Hepatic Artery Invasion and Pathological Invasion

	pA0	pA1	pA2	pA3	pA1/2/3	Total
fCurA/B						
CT-A0	29	0	0	0	0	29
CT-A1	10	0	0	1	1	11
CT-A2	0	0	0	0	0	0
CT-A3	1[a]	0	0	0	0	1
CT-A1/2/3	11	0	0	1	1	12
Total	40	0	0	1	1	41
fCurC						
CT-A0	3	0	0	0	0	3
CT-A1	8	0	2	0	2	10
CT-A2	1[a]	0	0	0	0	1
CT-A3	2[a]	0	0	0	0	2
CT-A1/2/3	11	0	2	0	2	13
Total	14	0	2	0	2	16

[a]Ipsilateral hepatic artery of the resected liver.

TABLE VIII. MDCT-Evaluated Hepatic Artery Invasion in Hilar Biliary Cancer

CT-A	n	Contralateral hepatic artery resection	pA0	pA123
Total	23	2	18	1
fCurA/B	12	2	10	1
CT-A0	1	1[a]	1	0
CT-A1				
Ipsilateral to resected liver	9	1[a]	8	1[b]
Contralateral to resected liver	1	0	ND	ND
CT-A2/3				
Ipsilateral to resected liver	1	0	1	0
Contralateral to resected liver	0	0	0	0
fCurC	11	0	8	1
CT-A0	1	0	1	0
CT-A1				
Ipsilateral to resected liver	5	0	4	1[b]
Contralateral to resected liver	2	0	ND	ND
CT-A2/3				
Ipsilateral to resected liver	3	0	3	0
Contralateral to resected liver	0	0	0	0

ND, not determined.
[a]pA0 at the resected contralateral hepatic artery.
[b]At ipsilateral hepatic artery of the resected liver.

invasion [31,32]. In biliary cancer, portal invasion is not a prognostic factor [33], and suspected arterial invasion is indicative of poor prognosis and a criterion for neoadjuvant chemoradiation. Thus, our findings should have an impact on the diagnosis-related decision-making regarding treatment strategy.

In this study, we evaluated MDCT just before surgery and after percutaneous transhepatic portal vein embolization (PTPE) in the patients who required this procedure (n = 11). The latter was provided to improve liver regeneration, which impacts the rate of curative (fA/B, R0) resection and prognosis of patients. For actual analysis of intention-to-treat at the first contact and after the decision for surgery, we should include information obtained before PTPE.

In conclusion, the present study demonstrated that suspected arterial invasion, as detected by MDCT, could predict poor prognosis of patients with biliary cancer after surgery. Suspected arterial invasion was a non-curative surgical factor associated with positive surgical margin. This MDCT-based preoperative factor could be useful for clinical decision-making regarding neoadjuvant therapy in combination with surgery.

REFERENCES

1. Japanese Society of Biliary Surgery. Classification of biliary tract carcinoma, 5th edition. Tokyo: Kanehara; 2003.
2. Miyakawa S, Ishihara S, Horiguchi A, et al.: Biliary tract cancer treatment: 5,584 results from the Biliary Tract Cancer Statistics Registry from 1998 to 2004 in Japan. J Hepatobiliary Pancreat Surg 2009;16:1–7.
3. Baek SY, Sheafor DH, Keogan MT, et al.: Two-dimensional multiplanar and three-dimensional volume-rendered vascular CT in pancreatic carcinoma: Interobserver agreement and comparison with standard helical techniques. AJR Am J Roentgenol 2001; 176:1467–1473.
4. Okumoto T, Sato A, Yamada T, et al.: Correct diagnosis of vascular encasement and longitudinal extension of hilar cholangiocarcinoma by four-channel multidetector-row computed tomography. Tohoku J Exp Med 2009;217:1–8.
5. Choi JY, Kim MJ, Lee JM, et al.: Hilar cholangiocarcinoma: Role of preoperative imaging with sonography, MDCT, MRI, and direct cholangiography. AJR Am J Roentgenol 2008;191:1448–1457.
6. Watadani T, Akahane M, Yoshikawa T, et al.: Preoperative assessment of hilar cholangiocarcinoma using multidetector-row CT: Correlation with histopathological findings. Radiat Med 2008;26:402–407.
7. Li J, Kuehl H, Grabellus F, et al.: Preoperative assessment of hilar cholangiocarcinoma by dual-modality PET/CT. J Surg Oncol 2008;98:438–443.
8. Unno M, Okumoto T, Katayose Y, et al.: Preoperative assessment of hilar cholangiocarcinoma by multidetector row computed tomography. J Hepatobiliary Pancreat Surg 2007;14:434–440.
9. Lee HY, Kim SH, Lee JM, et al.: Preoperative assessment of resectability of hepatic hilar cholangiocarcinoma: Combined CT and cholangiography with revised criteria. Radiology 2006;239: 113–121.
10. Kalra N, Suri S, Gupta R, et al.: MDCT in the staging of gallbladder carcinoma. AJR Am J Roentgenol 2006;186:758–762.
11. Furukawa H, Sano K, Kosuge T, et al.: Hilar cholangiocarcinoma evaluated by three-dimensional CT cholangiography and rotating cine cholangiography. Hepatogastroenterology 2000;47: 615–620.
12. Chen HW, Pan AZ, Zhen ZJ, et al.: Preoperative evaluation of resectability of Klatskin tumor with 16-MDCT angiography and cholangiography. AJR Am J Roentgenol 2006;186:1580–1586.
13. Otto G, Romaneehsen B, Hoppe-Lotichius M, et al.: Hilar cholangiocarcinoma: Resectability and radicality after routine diagnostic imaging. J Hepatobiliary Pancreat Surg 2004;11:310–318.
14. Ishikawa O, Ohigashi H, Sasaki Y, et al.: Intraoperative cytodiagnosis for detecting a minute invasion of the portal vein during pancreatoduodenectomy for adenocarcinoma of the pancreatic head. Am J Surg 1998;175:477–481.
15. Li J, Kuehl H, Grabellus F, et al.: Preoperative assessment of hilar cholangiocarcinoma by dual-modality PET/CT. J Surg Oncol 2008;98:438–443.
16. Furukawa H, Ikuma H, Asakura-Yokoe K, et al.: Preoperative staging of biliary carcinoma using 18F-fluorodeoxyglucose PET: Prospective comparison with PET+CT, MDCT and histopathology. Eur Radiol 2008;18:2841–2847.
17. Petrowsky H, Wildbrett P, Husarik DB, et al.: Impact of integrated positron emission tomography and computed tomography on staging and management of gallbladder cancer and cholangiocarcinoma. J Hepatol 2006;45:43–50.
18. Yasukawa T, Yoshikawa K, Aoyagi H, et al.: Usefulness of PET with 11C-methionine for the detection of hilar and mediastinal lymph node metastasis in lung cancer. J Nucl Med 2000;41:283–290.

19. Okami J, Dohno K, Sakon M, et al.: Genetic detection for micrometastasis in lymph node of biliary tract carcinoma. Clin Cancer Res 2000;6:2326–2332.
20. Marubashi S, Dono K, Nagano H, et al.: Detection of AFP mRNA-expressing cells in the peripheral blood for prediction of HCC recurrence after living donor liver transplantation. Transpl Int 2007;20:576–582.
21. Miyamoto A, Nagano H, Sakon M, et al.: Clinical application of quantitative analysis for detection of hematogenous spread of hepatocellular carcinoma by real-time PCR. Int J Oncol 2001;18: 527–532.
22. Miyamoto A, Fujiwara Y, Sakon M, et al.: Development of a multiple-marker RT-PCR assay for detection of micrometastases of hepatocellular carcinoma. Dig Dis Sci 2000;45:1376–1382.
23. André T, Reyes-Vidal JM, Fartoux L, et al.: Gemcitabine and oxaliplatin in advanced biliary tract carcinoma: A phase II study. Br J Cancer 2008;99:862–867.
24. Koeberle D, Saletti P, Borner M, et al.: Patient-reported outcomes of patients with advanced biliary tract cancers receiving gemcitabine plus capecitabine: A multicenter, phase II trial of the Swiss Group for Clinical Cancer Research. J Clin Oncol 2008; 26:3702–3708.
25. Furuse J, Takada T, Miyazaki M, et al.: Guidelines for chemotherapy of biliary tract and ampullary carcinomas. J Hepatobiliary Pancreat Surg 2008;15:55–62.
26. Iyer RV, Gibbs J, Kuvshinoff B, et al.: A phase II study of gemcitabine and capecitabine in advanced cholangiocarcinoma and carcinoma of the gallbladder: A single-institution prospective study. Ann Surg Oncol 2007;14:3202–3209.
27. Valle JW, Wasan H, Johnson P, et al.: Gemcitabine alone or in combination with cisplatin in patients with advanced or metastatic cholangiocarcinomas or other biliary tract tumours: A multicentre randomised phase II study—The UK ABC-01 Study. Br J Cancer 2009;101:621–627.
28. Kamisawa T, Tu Y, Egawa N, et al.: Thermo-chemo-radiotherapy for advanced bile duct carcinoma. World J Gastroenterol 2005; 11:4206–4209.
29. Brunner TB, Schwab D, Meyer T, et al.: Chemoradiation may prolong survival of patients with non-bulky unresectable extrahepatic biliary carcinoma. A retrospective analysis. Strahlenther Onkol 2004;180:751–757.
30. Sudan D, DeRoover A, Chinnakotla S, et al.: Radiochemotherapy and transplantation allow long-term survival for nonresectable hilar cholangiocarcinoma. Am J Transplant 2002;2: 774–779.
31. Ohigashi H, Ishikawa O, Eguchi H, et al.: Feasibility and efficacy of combination therapy with preoperative full-dose gemcitabine, concurrent three-dimensional conformal radiation, surgery, and postoperative liver perfusion chemotherapy for T3-pancreatic cancer. Ann Surg 2009;250:88–95.
32. Evans DB, Varadhachary GR, Crane CH, et al.: Preoperative gemcitabine-based chemoradiation for patients with resectable adenocarcinoma of the pancreatic head. J Clin Oncol 2008;26: 3496–3502.
33. Ebata T, Nagino M, Kamiya J, et al.: Hepatectomy with portal vein resection for hilar cholangiocarcinoma: Audit of 52 consecutive cases. Ann Surg 2003;238:720–727.

Evaluation of a New Immunoassay for Therapeutic Drug Monitoring of Tacrolimus in Adult Liver Transplant Recipients

Shigeru Marubashi, MD, PhD, Hiroaki Nagano, MD, PhD, Shogo Kobayashi, MD, PhD, Hidetoshi Eguchi, MD, PhD, Yutaka Takeda, MD, PhD, Masahiro Tanemura, MD, PhD, Koji Umeshita, MD, PhD, Morito Monden, MD, PhD, Yuichiro Doki, MD, PhD, and Masaki Mori, MD, PhD

Therapeutic drug monitoring is necessary when using tacrolimus (FK) due to the associated side effects. The aim of this study was to compare the chemiluminescent assay (CMIA) system with the previously established Abbott IMx Tacrolimus II microparticle enzyme immunoassay (MEIA) in liver transplant recipients and evaluate its accuracy. Between March and June 2008, all blood samples from the liver transplant recipients at the hospital were tested for FK trough level using 2 different methods, CMIA and MEIA. The posttransplant time, hematocrit, and other clinical parameters during the study period were recorded. FK trough level was analyzed in 398 samples from 57 liver transplant recipients by CMIA and MEIA. The correlation in FK level between the 2 methods was excellent ($r^2 = 0.941$). However, the FK level was underestimated in MEIA by more than 23% in samples with an FK level of less than 3.5 ng/mL and by 6.8% in those with an FK level between 3.5 and 5 ng/mL. CMIA is superior to MEIA in measuring low FK level, allowing the FK level to be maintained at less than 5 ng/mL in selected liver transplant recipients. The effects of maintaining low levels of FK should be evaluated in liver transplant recipients.

Keywords: *tacrolimus; liver transplantation; therapeutic drug monitoring; immunoassay*

Journal of Clinical Pharmacology, 2010;50:705-709

Tacrolimus (FK) is a potent immunosuppressant known as a calcineurin inhibitor and a key drug used in organ transplantation. FK is effective in preventing rejection and maintaining organ function in liver transplantation, but its side effects, such as nephrotoxicity,[1] diabetes mellitus,[2] hypertension, and infection, are life threatening in posttransplant management.[3] Therefore, therapeutic drug monitoring is necessary for transplant recipients to secure a better posttransplant course. Reduced exposure to elevated blood concentrations of tacrolimus provides adequate immunosuppression and improved renal function in kidney transplantation.[4] In liver transplant recipients, tacrolimus concentration should be minimized, especially in stable recipients after transplantation.

The IMx Tacrolimus II microparticle enzyme immunoassay (MEIA; Abbott Laboratories, Abbott Park, Illinois) is a standard system for monitoring tacrolimus blood concentrations.[5] However, the reported limit of quantification (LOQ) in blood concentration of tacrolimus using MEIA is 4.1 ng/mL,[6] which may be high and harmful in stable liver transplant recipients. A trough level of tacrolimus around 3 to 4 ng/mL seems adequate and could be reduced to even perhaps around 1 ng/mL.[6] A once-a-day tacrolimus dose would require a target level as low as around 1 ng/mL, although the MEIA system does not support such low levels.

The newly developed ARCHITECT tacrolimus assay using the automated chemiluminescent assay (CMIA; Abbott Laboratories) for quantitative measurement of tacrolimus on the ARCHITECT i2000SR platform is highly sensitive and provides precise

From the Department of Surgery, Osaka University, Graduate School of Medicine, Suita, Osaka, Japan. Submitted for publication May 1, 2009; revised version accepted September 24, 2009. Address for correspondence: Shigeru Marubashi, MD, PhD, Department of Surgery, Osaka University Graduate School of Medicine, 2-2 YAMADAOKA, SUITA City, Osaka 565-0871, Japan; e-mail: smarubashi@gesurg.med.osaka-u.ac.jp.
DOI:10.1177/0091270009352188

measurement. It also allows the management of low-target concentrations in liver transplant recipients.

To our knowledge, there are no reports that compare MEIA and CMIA in the assessment of tacrolimus in liver transplant recipients. The present study was designed to compare these 2 methods in liver transplant recipients and determine the efficacy of the ARCHITECT tacrolimus assay in clinical settings.

PATIENTS AND METHODS

Abbott IMx Tacrolimus II Microparticle Enzyme Immunoassay

In this immunoassay, whole-blood sample is mixed with the microparticle reagent, followed by incubation, in which tacrolimus in the sample binds to the antibody binding sites on the microparticles. An aliquot of the mixture is then transferred to a glass-fiber filter, and tacrolimus-alkaline phosphatase conjugate is added to the filter. Conjugates that do not bind to the remaining antibody binding sites on the microparticles are removed by washing. Then, the substrate reagent is added to the filter and the rate of appearance of the fluorescence product is measured by front surface fluorescence measurements. The rate is inversely proportional to the amount of the analyte present in the patient sample or standard.

Automated CMIA for the Quantitative Determination of Tacrolimus on the ARCHITECT i2000SR Platform

The CMIA method is based on the enzyme immunoassay (EIA) principle. In contrast to the EIA, where the antigen-antibody complexes are detected by enzyme-labeled conjugate, the CMIA uses an acridinium-labeled conjugate as the detection system. The LOQ of blood concentration of tacrolimus using CMIA is as low as 0.8 ng/mL.[6]

Comparison of MEIA and CMIA

During the study period from March to June 2008, peripheral blood samples from 57 liver transplant recipients were analyzed by both techniques. Among 57 recipients, 44 patients underwent living donor liver transplantation, and 13 received deceased donor liver transplantation.

All recipients were taking tacrolimus (Prograf) every 12 hours, and blood samples were obtained at trough level. Each blood sample was divided into 2 portions and each used immediately for 1 assay. The immunosuppressive protocol consisted of tacrolimus and steroid with or without mycophenolate mofetil (MMF) or tacrolimus and anti-CD25 monoclonal antibody with MMF. Tacrolimus was started at a dose of 0.03 mg/kg and titrated 8 to 12 ng/mL as trough level during the first 3 weeks after transplant, then reduced to 6 to 8 ng/mL in the first 3 months and 4 to 6 ng/mL thereafter.

The ARCHITECT ratio (AR) was defined as [C(ARCHITECT) – C(IMx)]/C(ARCHITECT), where C(ARCHITECT) is FK trough concentration in the CMIA method, and C(IMx) is that in the MEIA method. Samples were also divided according to hematocrit into <25%, 25% to 45%, and over 45%.

Statistical Analysis

Results are expressed as mean ± standard deviation or median. Statistical examination of the correlations was based on the Pearson product-moment correlation. A P value less than .05 was considered statistically significant.

RESULTS

Samples from 57 liver transplant recipients (43 living donor liver transplantation and 14 deceased donor liver transplantation), including 3 patients who received liver transplantation during the study period, were analyzed (Table I). Time after liver transplantation ranged from 0 to 7.7 years (3.5 ± 2.2 years). The primary diagnoses of these 57 patients are listed in Table I. The total number of blood samples analyzed by the 2 methods was 398, including 35 samples within 3 weeks after liver transplantation, 57 samples between 3 weeks and 3 months, 93 samples between 3 months and 1 year, and 213 samples over 1 year. FK trough level was 11.9 ± 3.1 (MEIA), 11.5 ± 2.8 (CMIA) within 3 weeks; 11.3 ± 3.2 (MEIA), 10.8 ± 2.8 (CMIA) between 3 weeks and 3 months; 8.2 ± 4.5 (MEIA), 8.0 ± 4.1 (CMIA) between 3 months and 1 year; and 6.4 ± 3.3 (MEIA), 6.5 ± 2.9 (CMIA) over 1 year.

FK trough level ranged from 0.2 to 23.0 ng/mL in the MEIA method and from 1.4 to 21.9 in the CMIA method. The FK level in all samples was above the LOQ in the CMIA method (0.8 ng/mL), whereas 13.4% of all samples were below the LOQ (4.1 ng/mL) in the MEIA method. Samples with hematocrit less than 25% accounted for 4.0% (n = 16), whereas

Table I Patients' Characteristics

Number of patients	57
Sex (male/female)	34/23
Age, y, mean ± SD (range)	47.4 ± 14.7 (19-67)
Type of liver transplant, n	
Deceased donor	14
Living donor	43
Primary diagnosis	
Hepatitis C virus cirrhosis	22
Hepatitis B virus cirrhosis	8
Primary biliary cirrhosis	8
Primary sclerosing cholangitis	3
Alcohol cirrhosis	3
Wilson disease	2
Biliary atresia	3
Budd-Chiari syndrome	1
Citrullinemia	1
Cryptogenic	2
Fulminant hepatic failure	4
Months posttransplantation, mean ± SD (range)	41.8 ± 26.5 (0-92.4)
New transplantation, n (%)	3 (5.3)
Within 12 months posttransplantation, n (%)	9 (15.8)
12 to 36 months posttransplantation, n (%)	20 (35.1)
Over 36 months posttransplantation, n (%)	25 (43.9)

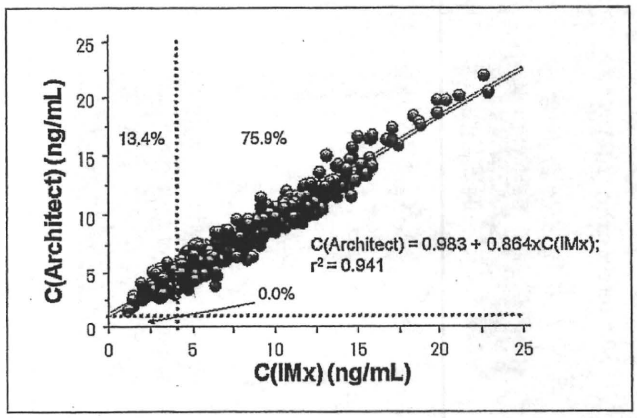

Figure 1. Correlation of tacrolimus (FK) trough concentrations measured by the microparticle enzyme immunoassay (MEIA) and chemiluminescent assay (CMIA) methods. The association between the 2 methods was excellent. C(ARCHITECT) = 0.983 + 0.864 × C(IMx); r^2 = 0.941. C(ARCHITECT) is the FK trough concentration measured by the CMIA method; C(IMx) is the FK trough concentration measured by the MEIA method. Of all samples, 13.4% were below the limit of quantification (4.1 ng/mL) in the MEIA method, whereas all samples were within the limit of qualification in the CMIA method.

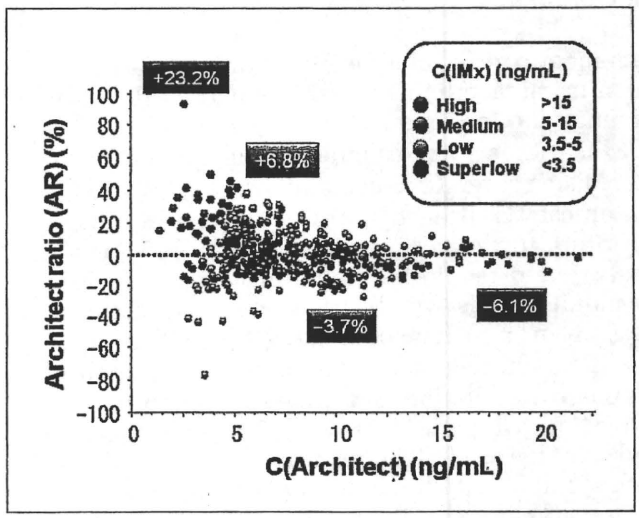

Figure 2. Correlation of tacrolimus trough concentration measured by the microparticle enzyme immunoassay (MEIA) and chemiluminescent assay (CMIA) methods using the ARCHITECT ratio (AR). The mean AR was 23.2% in samples with tacrolimus (FK) level less than 3.5 ng/mL and 6.8% in samples with FK level between 3.5 and 5 ng/mL, as measured by the MEIA. AR was defined as [C(ARCHITECT) – C(IMx)]/C(ARCHITECT).

those with hematocrit more than 45% accounted for 7.5% (n = 30).

The association between the 2 methods showed excellent correlation (Figure 1). C(ARCHITECT) = 0.983 + 0.864 × C(IMx); r^2 = 0.941. However, the discrepancy in the FK level between the 2 methods in terms of AR was large in samples with low FK level, especially less than 5 ng/mL. AR was 23.2% in samples with FK level less than 3.5 ng/mL (MEIA) and 6.8% in samples with FK level between 3.5 and 5 ng/mL (MEIA) (Figure 2). In contrast, there was excellent correlation between the 2 methods, with AR –3.7% (FK level between 5 and 15 ng/mL) and –6.1% (FK level over 15 ng/mL; Figure 2).

Analysis of the effect of hematocrit on FK level showed that the CMIA-MEIA discrepancy was larger in samples with low hematocrit (<25%), AR = –12.8%, as well as in samples with high hematocrit (>45%), AR = 11.4% (Figure 3).

In 14 of the 57 patients, the dose of FK was reduced due to renal dysfunction in 2 patients and stable graft function with more than 2 years after liver transplantation in 12 patients. The follow-up period in these 14 patients was 4.4 ± 1.8 years (range, 2.1-6.2 years). None of the patients in this study showed signs of rejection.

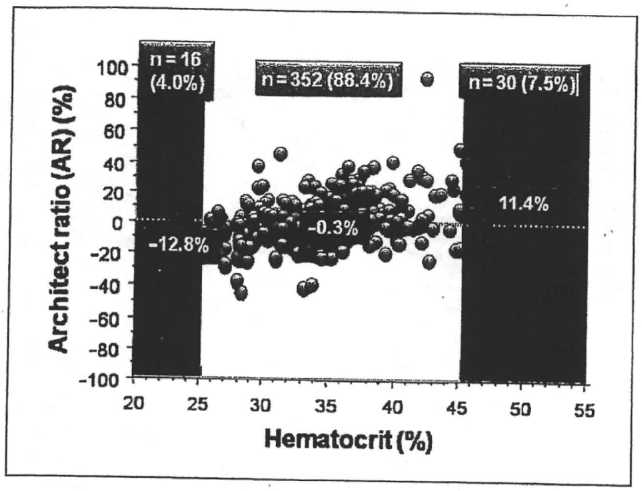

Figure 3. Correlation of ARCHITECT ratio (AR) with hematocrit (n = 398). The discrepancy in tacrolimus (FK) level measured by the chemiluminescent assay (CMIA) and microparticle enzyme immunoassay (MEIA) methods was larger in samples with low hematocrit (<25%, AR = –12.8%) and also in samples with high hematocrit (>45%, AR = 11.4%). AR was defined as [C(ARCHITECT) – C(IMx)]/C(ARCHITECT).

DISCUSSION

Therapeutic drug monitoring (TDM) is necessary when using tacrolimus due to the narrow therapeutic range and to minimize the side effects. The ideal TDM is estimated by calculating the area under the curve using several FK levels such as C0, C2, and C6. The efficacy C0 (trough) monitoring makes a suitable substitute to the AUC as it is simple and easy to measure and requires a single measure. Therefore, C0 monitoring is widely used and is an accepted measure in most transplant programs. Other methods of monitoring tacrolimus include detection of calcineurin inhibition and mixed lymphocyte reaction (MLR), which are more complex and difficult to apply in daily clinical practice. Other candidate methods for TDM include the cylex Immuknow assay, cytokines (eg, interleukin [IL]-5, IL-2, interferon [IFN]-γ, IFN-α, IL-2 receptor), neopterin, serum amyloid A, and lymphotoxin,[7,8] although their clinical application has not been established yet due to inadequate evidence of suitability for TDM.

Accurate detection of tacrolimus level in liver transplant recipients is important; however, the limitation of detecting low concentrations of tacrolimus has hampered efforts to lower the target FK level in stable liver transplant recipients. The LOQ of currently available MEIA in our hospital is 4.1 ng/mL, but we frequently encounter liver transplant recipients with normal liver function who show no sign of rejection and in whom the FK trough level is about 3.5 ng/mL. The LOQ in the CMIA method is as low as ~1 ng/mL. In our study, we maintained the FK trough level at less than 3.5 ng/mL in 13.4% liver transplant recipients.

Comparison of these 2 methods showed that the FK level varies in 2 manners. One factor relates to the hematocrit level. In the MEIA method, it has been known that there could be a substantial error in patients with low or high hematocrit.[9,10] In contrast, there is minimal error in relation to the hematocrit level in the CMIA method (Figure 3). Thus, it is likely that the discrepancy in the results of the 2 methods is due to the shortfall in the MEIA method. The more important second factor is the FK level itself. The correlation between the 2 methods was excellent at the high FK level (ie, >5 ng/mL), whereas the discrepancy between the values obtained by the 2 methods increased in samples of patients with low FK level (ie, <5 ng/mL). The FK level was underestimated, and the discrepancy ratio was more than 23% by the MEIA method at FK levels <3.5 ng/mL but was 6.8% at FK levels between 3.5 and 5 ng/mL (Figure 2). Thus, the MEIA method has a substantial error when FK level is <5 ng/mL, whereas the CMIA method is relatively accurate even in the range of 1 to 5 ng/mL.

Accurate measurement of serum FK level is necessary for TDM of FK, especially during long-term and stable periods after liver transplantation. Maintaining low FK level in stable liver transplant recipients could result in a better preservation of kidney function and less side effects such as infection, hypertension, diabetes, and hyperlipidemia. It would be useful to use once-a-day FK tablet, where lower FK trough level might be effective in avoiding rejection.

Several other methods are available for measurement of FK level in addition to CMIA and MEIA, such as the enzyme-multiplied immunoassay technique (EMIT), high-performance liquid chromatography with ultraviolet detection (HPLC-UV), and most recently mass spectrometry. Although the relationship between CMIA method and methods other than MEIA has not yet been investigated using clinical samples, to date, the CMIA method is the most accurate and clinically useful for real-time TDM of tacrolimus in liver transplant recipients.

CONCLUSIONS

We conclude based on the results of the present study that the CMIA method is superior to the

MEIA method for measurement of serum FK level, especially low FK levels (<5 ng/mL). Using this method, we can investigate the effects of low FK level in terms of reducing the chance of various short- and long-term side effects in liver transplant recipients.

We thank M. Mukaida, N. Hata, and S. Iyama (Department of Medical Technology, Osaka University Hospital) for performing the immunoassays.

REFERENCES

1. Gonwa TA, Mai ML, Melton LB, et al. End-stage renal disease (ESRD) after orthotopic liver transplantation (OLTX) using calcineurin-based immunotherapy: risk of development and treatment. *Transplantation.* 2001;72:1934-1939.

2. Drachenberg CB, Klassen DK, Weir MR, et al. Islet cell damage associated with tacrolimus and cyclosporine: morphological features in pancreas allograft biopsies and clinical correlation. *Transplantation.* 1999;68:396-402.

3. First MR. Tacrolimus based immunosuppression. *J Nephrol.* 2004;17(suppl 8):S25-S31.

4. Ekberg H, Tedesco-Silva H, Demirbas A, et al. Reduced exposure to calcineurin inhibitors in renal transplantation. *N Engl J Med.* 2007;357:2562-2575.

5. Grenier FC, Luczkiw J, Bergmann M, et al. A whole blood FK 506 assay for the IMx analyzer. *Transplant Proc.* 1991;23:2748-2749.

6. Amann S, Parker TS, Levine DM. Evaluation of 2 immunoassays for monitoring low blood levels of tacrolimus. *Ther Drug Monit.* 2009;31:273-276.

7. Dumont RJ, Ensom MH. Methods for clinical monitoring of cyclosporin in transplant patients. *Clin Pharmacokinet.* 2000; 38:427-447.

8. Staatz CE, Tett SE. Clinical pharmacokinetics and pharmacodynamics of tacrolimus in solid organ transplantation. *Clin Pharmacokinet.* 2004;43:623-653.

9. Armendariz Y, Garcia S, Lopez RM, Pou L. Hematocrit influences immunoassay performance for the measurement of tacrolimus in whole blood. *Ther Drug Monit.* 2005;27:766-769.

10. Bouzas L, Ortega FJ, Casado P, et al. Effect of the hematocrit and its correction on the relationship between blood tacrolimus concentrations obtained using the microparticle enzyme immunoassay (MEIA) and enzyme multiplied immunoassay technique (EMIT). *Clin Lab.* 2007;53:591-596.